

Nuclear accumulation of Smad complexes occurs only after the midblastula transition in *Xenopus*

Yasushi Saka^{1,2,*}, Anja I. Hagemann^{1,*}, Olaf Piepenburg^{1,†} and James C. Smith^{1,‡}

Activin and the Nodal-related proteins induce mesendodermal tissues during *Xenopus* development. These signals act through specific receptors to cause the phosphorylation, at their carboxyl termini, of Smad2 and Smad3. The phosphorylated Smad proteins form heteromeric complexes with Smad4 and translocate into the nucleus to activate the transcription, after the midblastula transition, of target genes such as *Xbra* and *gooseoid* (*gsc*). In this paper we use bimolecular fluorescence complementation (BiFC) to study complex formation between Smad proteins both in vivo and in response to exogenous proteins. The technique has allowed us to detect Smad2-Smad4 heteromeric interactions during normal *Xenopus* development and Smad2 and Smad4 homo- and heteromers in isolated *Xenopus* blastomeres. Smad2-Smad2 and Smad2-Smad4 complexes accumulate rapidly in the nuclei of responding cells following Activin treatment, whereas Smad4 homomeric complexes remain cytoplasmic. When cells divide, Smad2-Smad4 complexes associate with chromatin, even in the absence of ligand. Our observation that Smad2-Smad4 complexes accumulate in the nucleus only after the midblastula transition, irrespective of the stage at which cells were treated with Activin, may shed light on the mechanisms of developmental timing.

KEY WORDS: *Xenopus*, Smads, Activin, Nodal-related proteins, Bimolecular fluorescence complementation, Midblastula transition

INTRODUCTION

The TGF β family of growth factors, including Activin and the Nodal-related proteins, plays roles in the regulation of cell proliferation, differentiation and migration in the embryos and adults of vertebrate and invertebrate species (Shen, 2007). TGF β family members signal by binding to type II serine-threonine kinase receptors, which then associate with, and phosphorylate, type I receptors. The activated type I receptors go on to phosphorylate receptor-regulated Smad proteins (R-Smads, including Smad1, Smad2, Smad3, Smad5 and Smad8) and these in turn associate with Smad4, accumulate in the nucleus, and regulate the expression of downstream target genes, usually by interacting with a specific cofactor.

Activin and the *Xenopus* Nodal-related proteins (Xnrs) induce formation of the mesendoderm during early *Xenopus* development (Heasman, 2006). Although one can visualise the dynamic spatial and temporal regulation of Activin/Xnr signalling by use of an antibody that recognises the phosphorylated form of Smad2 (Schohl and Fagotto, 2002), this technique involves the use of serial cryosections of embryos at different stages of development and does not permit true real-time analysis. To address this point, and to allow one to monitor Smad signalling in other cells and tissues, we have investigated whether bimolecular fluorescence complementation (BiFC) (Hu et al., 2002) might provide an alternative approach to monitor Smad signalling. BiFC takes advantage of the fact that when the two non-fluorescent amino- and carboxyl-terminal fragments of yellow fluorescent protein (YFP)

are brought into close apposition they interact to form a fluorescent protein. We have optimised this technique for use in the highly autofluorescent *Xenopus* embryo by using mutated versions of VENUS, and thereby succeeded in detecting homomeric interactions between two Smad2 and two Smad4, as well as heteromeric complex formation between Smad2 and Smad4. Importantly, our approach is at least semi-quantitative, and will allow us to monitor Smad signalling during the normal development of *Xenopus*. Interestingly, we note that during mitosis Smad complexes associate with chromatin; this may provide a mechanism for the equal distribution of Smad proteins at cell division.

Finally, we note that the nuclear accumulation of Smad2-Smad4 complexes in response to induction only occurs after the midblastula transition, irrespective of the stage at which cells are exposed to Activin. This observation may help shed light on the complex problem of developmental timing in the early *Xenopus* embryo.

MATERIALS AND METHODS

Xenopus embryo manipulation

Fertilisation and culture of *Xenopus* embryos were as described previously (Tada et al., 1997). They were staged according to Nieuwkoop and Faber (Nieuwkoop and Faber, 1994). Animal cap cells were dissociated in Ca²⁺- and Mg²⁺-free medium (75 mM Tris pH 7.5, 880 mM NaCl, 10 mM KCl, 24 mM NaHCO₃) for 30-45 minutes at room temperature before treating with Activin.

Western blotting

Fertilized eggs were injected with the relevant RNA at the one-cell stage (see figure legends for details) and animal caps were dissected at blastula stages 8 to 9. Protein extracts were prepared from the animal caps as described previously (Saka and Smith, 2004) and the equivalent of 10 animal caps was applied to each lane of a SDS polyacrylamide gel before blotting onto Hybond P membrane (Amersham Bioscience). Antibodies used were anti-Smad2/3 (rabbit IgG, from Cell Signaling, 1:1000) or anti-phospho-Smad2 (monoclonal rabbit IgG from Cell Signaling, 1:1000). HRP-conjugated secondary antibodies were anti-rabbit IgG (whole antibody, Amersham, 1:1000; or Santa Cruz, 1:4000).

¹Wellcome Trust/Cancer Research UK Gurdon Institute and Department of Zoology, University of Cambridge, Tennis Court Road, Cambridge CB2 1QN, UK.

²Interdisciplinary Research Institute and Institut de Biologie de Lille, 1 rue du professeur Calmette, BP447, 59021 Lille Cedex, France.

*These authors contributed equally to this work

[†]Present address: ASM Scientific Ltd, Building 405, Babraham Research Campus, Babraham CB2 4AT, UK

[‡]Author for correspondence (e-mail: jim@gurdon.cam.ac.uk)

BiFC constructs, mRNA injection and transfection of mammalian cells

The N-terminal and C-terminal halves of VENUS (Nagai et al., 2002) were amplified by PCR and cloned into pCS2+. VENUS fragments were fused to the N terminus of human SMAD4 with an 11 amino acids linker (TGGGGGGGGGG) or to the N terminus of *Xenopus* Smad2 with a four amino acids linker (TGSS). For the constructs VC155-Smad3 and VC155-Smad2 Δ exon3, Smad2 was replaced either by *Xenopus* Smad3 (a gift from Caroline Hill, Cancer Research UK London Research Institute, London, UK) or *Xenopus* Smad2 Δ exon3 (a gift from Oliver Nentwich, Gurdon Institute, Cambridge, UK). Site-directed mutagenesis to create modified forms of VENUS was performed as described previously (Sawano and Miyawaki, 2000). VENUS, mRFP1, ECFP, ECFP-GPI, ECFP-NLS, histone H2B-ECFP and Emerin-ECFP were all cloned into the expression vector pCS2+ and checked by sequencing. GFP-emerin was a kind gift from Chris Hutchison (Durham University, Durham, UK), YFP-histone H2B, a kind gift from Andrea Brand (Gurdon Institute, Cambridge, UK) and the NLS sequence a kind gift from Steve Jackson (Gurdon Institute, Cambridge, UK).

All constructs in pCS2+ were linearised with *NotI* and transcribed in vitro using SP6 RNA polymerase and the mMESSAGE mMACHINE kit (Ambion). HEK293T cells were cultured in D-MEM medium (high glucose without sodium pyruvate; Gibco 41965-039) with 10% serum and transfected with 0.5–2 μ g of each plasmid DNA using Lipofectamine 2000 (Invitrogen).

Real-time PCR

Total RNA was prepared from 15 animal caps using the Trizol reagent (Invitrogen), followed by isopropanol precipitation. RNA was dissolved in water and used as template for real-time RT-PCR. Real-time RT-PCR with the LightCycler (Roche) was carried out using the manufacturer's RNA amplification kit. All determinations included a negative control. Primers specific for *Xbra*, goosecoid (*gsc*), chordin and ornithine decarboxylase were as described previously (Piepenburg et al., 2004). All values are normalised to the level of ornithine decarboxylase in each sample.

Imaging

Animal caps were dissociated in Ca²⁺- and Mg²⁺-free medium (CMFM) at the indicated stages. Dissociated cells were seeded onto a fibronectin-coated glass bottom dish (MatTek) in 0.75% normal amphibian medium (NAM) with 0.2% BSA and with or without 16 U/ml Activin (Cooke et al., 1987). The image in Fig. 1 was taken using a Leica MZ FLIII dissecting microscope equipped with RFP and YFP filters. The image in Fig. 3 was taken using a Leica DM IRB inverted fluorescence microscope with a Hamamatsu ORCA ER camera and analysed with Open Lab software. Fig. 3C, Figs 4, 5, 6 and Fig. S1 (see Fig. S1 in the supplementary material) images were taken using a Perkin Elmer Spinning Disk confocal microscope with a Zeiss Axiovert 200M inverted microscope and a Hamamatsu ORCA ER camera. CFP protein was excited at 440 nm and VENUS BiFC at 514 nm. Pictures were taken with Ultra View ERS software. All confocal pictures are taken with a 40 \times objective and represent a merged z-stack comprising 15 slices of 1 μ m each.

RESULTS

BiFC in *Xenopus*

The application of fluorescence techniques in *Xenopus* is hampered by high levels of autofluorescence deriving from yolk platelets. In an effort to improve the BiFC signal-to-noise ratio we therefore turned, like others (Shyu et al., 2006), to VENUS, a variant of enhanced yellow fluorescent protein (EYFP) which is less sensitive to pH and chloride ion concentration than EYFP and which matures more rapidly (Nagai et al., 2002). We chose two positions, both located within a loop between two β -sheets, to divide VENUS into two fragments: immediately after N144 or immediately after A154. The latter position was used in the original BiFC experiments using unmodified YFP (Hu et al., 2002); the former was used in the development of a fluorescent reagent to monitor Ca²⁺ levels in HeLa

cells (Nagai et al., 2001). We refer to the two types of VENUS N-terminal fragments as VN144 and VN154 and the two types of C-terminal fragments as VC145 and VC155.

In contrast to previous work using COS-1 cells (Shyu et al., 2006), we found that *Xenopus* embryos injected with as little as 50 pg of RNAs encoding either pair of complementary VN and VC fragments became fluorescent (Fig. 1A,D). No fluorescence was observed when the VN or VC fragments were expressed alone (data not shown). This apparent self-assembly of VENUS, which would significantly compromise its utility in BiFC experiments, may derive from the mutations introduced into EYFP that were designed to improve its folding and maturation (Nagai et al., 2002). To address this problem, mutations were introduced back into VENUS. Point mutation T153M is located at the junction between one of the β -strands and a loop in the crystal structure; it is likely to affect protein folding. The other mutations (L46F, L64F and Y203H) affect maturation of the chromophore (Rekas et al., 2002). Different combinations of N-terminal and C-terminal VENUS fragments carrying different combinations of mutations were tested for self-assembly by injecting RNAs into *Xenopus* embryos (Table 1). Out of 30 combinations, ten produced little fluorescence (Fig. 1B,E and data not shown). Of these, VNm9, a VN154 fragment carrying the

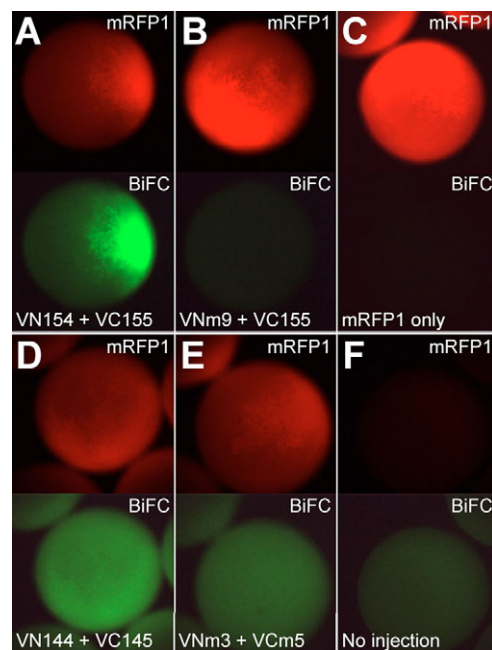


Fig. 1. Self-assembly of VENUS fragments is prevented by specific mutations. RNA encoding the indicated combinations of wild-type or mutated VENUS fragments (500 pg of each) was injected into *Xenopus* embryos at the one-cell stage in the presence of RNA encoding monomeric red fluorescent protein (mRFP1; 500 pg) as a lineage marker. Embryos were cultured to midblastula stage 9 and examined using a fluorescence dissecting microscope to visualise mRFP1 (top of each panel) or VENUS (bottom of each panel). (A) Strong fluorescence is observed following injection of mRNA encoding VN154 and VC155. (B) Mutation of VN154 to create VNm9 abolishes self-assembly and fluorescence. (C) Injection of mRFP1 alone. (D) Strong fluorescence is observed following injection of mRNA encoding VN144 and VC145. (E) VENUS fluorescence does not occur in embryos injected with RNA encoding VNm3 and VCm5 and only background level of fluorescence is observed. (F) An uninjected embryo illustrating background fluorescence.

Table 1. Optimisation of BiFC constructs

BiFC pair		Mutation				BiFC fluorescence	
N-terminal fragment	C-terminal fragment	L46F	L64F	T153M	Y203H	<i>Xenopus</i> cells	HEK293T cells
VN144	VC145					+	ND
VNm1	VC145	√				+	ND
VNm2	VC145		√			+	ND
VNm3	VC145	√	√			+	ND
VN144	VCm4			√		+	ND
VNm1	VCm4	√		√		+	ND
VNm2	VCm4		√	√		+	ND
VNm3	VCm4	√	√	√		+	ND
VN144	VCm5				√	+	ND
VNm1	VCm5	√			√	+	ND
VNm2	VCm5		√		√	+	ND
VNm3	VCm5	√	√		√	-	ND
VN144	VCm6			√	√	+	ND
VNm1	VCm6	√		√	√	+	ND
VNm2	VCm6		√	√	√	+	ND
VNm3	VCm6	√	√	√	√	-	ND
VN154	VC155					++	ND
VNm7	VC155	√				-	++
VNm8	VC155		√			-	++
VNm9	VC155			√		-	++
VNm10	VC155	√	√			-	±
VNm11	VC155	√		√		-	++
VNm12	VC155		√	√		-	++
VNm13	VC155	√	√	√		-	±
VN154	VCm14				√	-	ND
VNm7	VCm14	√			√	++	ND
VNm8	VCm14		√		√	+	ND
VNm9	VCm14			√	√	++	ND
VNm10	VCm14	√	√		√	+	ND
VNm11	VCm14	√		√	√	++	ND
VNm12	VCm14		√	√	√	+	ND
VNm13	VCm14	√	√	√	√	±	ND

ND, Not determined.

point mutation T153M, did not fluoresce in combination with VC155, and this combination of VENUS fragments was used in further studies. We note that constructs tagged with VN154 and VC155 tend to be more fluorescent than those tagged with VN144 and VC145 (compare Fig. 1A with Fig. 1D, and data not shown).

Smad2 and Smad4 BiFC constructs retain biological activity

Reagents designed to reveal the association of Smad2 with Smad4 were created by fusing VENUS fragments to the N termini of the two proteins (Fig. 2A). To confirm that such Smad constructs retain biological activity, capped RNA was injected into *Xenopus* embryos, and animal caps were dissected at late blastula stage 9 and cultured to the equivalent of the early gastrula or the late neurula stage, when they were monitored for the activation of *gsc* and *Xbra* (Cho et al., 1991; Smith et al., 1991) and then for the elongation or inversion movements that presage differentiation as mesoderm (Armes and Smith, 1997; Symes and Smith, 1987).

Animal pole regions derived from uninjected embryos or embryos injected with mRNAs encoding individual tagged Smad constructs expressed neither *Xbra* nor *gsc* at the early gastrula stage. However, strong expression of these genes was observed in caps derived from embryos injected with a combination of either HA- or VENUS-tagged forms of Smad2 and Smad4 (Fig. 2B), at levels comparable to those induced by injection of 5 pg Activin RNA (Fig. 2B). Such animal caps also underwent elongation (data not shown). These results indicate that Smad constructs carrying VNm9 or VC155 tags

at their N termini are able to interact with each other to induce the expression of their target genes. The inability of the individual tagged proteins to induce target gene expression at these low levels of injected RNA is likely to be due to limiting amounts of the complementary endogenous Smad protein.

Activin-induced nuclear accumulation of Smad complexes

To investigate whether tagged Smad constructs can reveal the ligand-induced association of Smad2 and Smad4 and thus signalling by members of the TGFβ family, such as Activin, *Xenopus* eggs were injected with RNA encoding VNm9-tagged Smad2 or Smad4, together with VC155-tagged Smad2 and, as a lineage tracer, mRFP1 (Campbell et al., 2002). Animal pole regions containing mRFP1 fluorescence were dissected at midblastula stage 8, and cells were dissociated and cultured to the equivalent of early gastrula stages 10-11 on a fibronectin-coated surface in the presence or absence of Activin. As a control for non-specific fluorescence we also injected a VC155-Smad2 construct that lacks the MH2 and linker regions of Smad2 as well as part of the MH1 domain (VC155-Smad2ΔC; Fig. 3A). This protein should not interact with Smad4 (Hata et al., 1997). Preliminary western blot analyses using VN154-Smad2 (which differs from VNm9-Smad2 by just one amino acid) confirmed that the truncated constructs are expressed at levels similar to those of the full-length proteins (data not shown) and experiments described below (Fig. 6E) indicate that levels of VN154-Smad2 resemble those of endogenous Smad2.

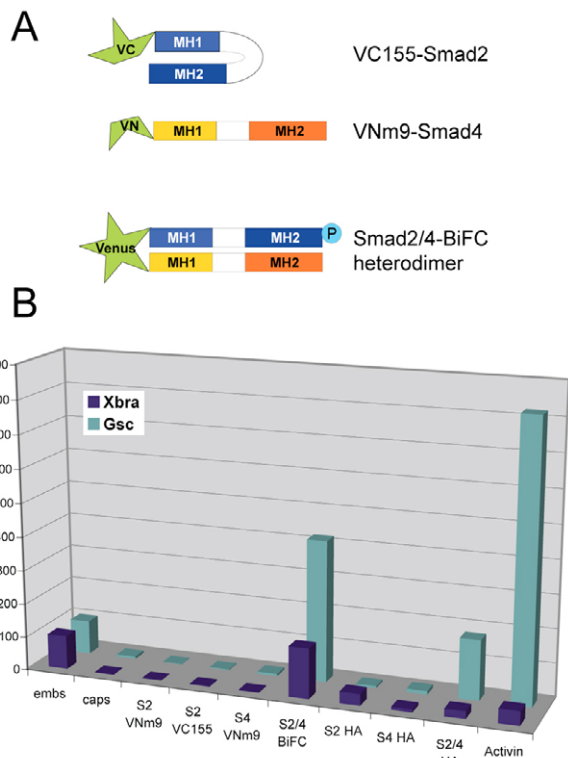


Fig. 2. Tagged forms of Smad2 and Smad4 retain their biological activities. (A) Illustration of the principle of bimolecular fluorescence. In unstimulated cells, in which Smad2 is not phosphorylated, Smad2 and Smad4 do not interact, and the N-terminal and C-terminal portions of VENUS are not able to complement. Phosphorylation of Smad2 results in a conformational change and allows interaction with Smad4 and fluorescence complementation. (B) Tagged Smad constructs retain their biological activity. *Xenopus* embryos received no injections (embs, caps), or were injected at the one cell stage with RNA encoding tagged forms of Smad2 or Smad4 proteins (100 pg for VC155-Smad2/VNm9-Smad4 BiFC tags and 80 pg for HA tags), alone or in combination, or with 5 pg RNA encoding Activin. Animal caps were dissected at the midblastula stage and cultured to the equivalent of early gastrula stage 10.5. Note that when expressed individually, tagged forms of Smads do not induce expression of *Xbra* and *gsc*, but co-expression of Smad2 and Smad4 (100 pg RNA of each) activates both genes at levels similar to those induced by Activin.

In the absence of Activin, we noted cytoplasmic fluorescence associated with the formation of Smad2-Smad2, Smad2-Smad4 and Smad4-Smad4 complexes (Fig. 3Ba,e,i and see Fig. 4A). Activin treatment of these animal cap cells caused detectable nuclear accumulation of Smad2-Smad2 complexes (Fig. 3Bb) and strong accumulation of Smad2-Smad4 complexes compared to levels of cytoplasmic fluorescence (Fig. 3Bf).

Injection of RNAs encoding VNm9-Smad4 and VC155-Smad4 into *Xenopus* embryos revealed that Smad4 proteins interact with each other as well as with Smad2 (Fig. 3Bi,j). Fluorescence was detected almost exclusively in the cytoplasm, both in the absence and the presence of Activin, suggesting that Smad4 homodimers represent an inactive state of Smad4.

As we discuss below, it is possible that interactions between Smad2 and Smad4 are stabilised by the BiFC technique. However, prolonged culture of Activin-treated animal pole blastomeres reveals that levels of BiFC fluorescence in the nucleus have decreased by

stage 13 (Fig. 3C), by which stage, levels of nuclear GFP-Smad2 and phospho-Smad2 have also declined (Faure et al., 2000; Grimm and Gurdon, 2002; Lee et al., 2001).

Subcellular localisation of Smad complexes

The subcellular localisation of Smad complexes as revealed by BiFC was further analysed by use of spinning disk confocal microscopy, which provides an improved signal-to-noise ratio. These experiments revealed that in the absence of ligand, Smad2-Smad4 fluorescence is associated with the cytoplasm and is enriched at the nuclear membrane (Fig. 4A). The distribution of Smad2-Smad4 complexes at the nuclear membrane was confirmed in experiments in which embryos were co-injected with RNA encoding ECFP-tagged emerin (Fig. 4B), an integral membrane protein that interacts with lamins A/C on the inner nuclear membrane (Bengtsson, 2007; Gruenbaum et al., 2005). Following Activin treatment the nucleus becomes particularly bright (Fig. 4C). There appears to be no consistent sub-nuclear distribution of BiFC fluorescence, although in some cells distinct spots can be made out (Fig. 4C arrows).

Spinning disk confocal microscopy revealed that all combinations of Smad dimers that have been tested, including Smad2-Smad2, Smad2-Smad4, Smad4-Smad4, Smad2 Δ exon3-Smad4 and Smad3-Smad4 (see Materials and methods) associate with chromosomes during mitosis, both in the presence and in the absence of ligand (Fig. 4D,E). This observation contrasts with data obtained using an antibody directed against Smad2, indicating that (presumably monomeric) Smad2 associates with the mitotic spindle (Batut et al., 2007; Dong et al., 2000). Both these phenomena may ensure the equal partition of Smad proteins and complexes between daughter cells.

The localisation of Smad-BiFC complexes to nuclear membrane and chromosomes appears to be specific; injection of 200 pg RNA encoding the complementary VENUS fragments VC155 and VNm9 (representing a 20-fold molar excess over the levels used elsewhere in this investigation) does not cause fluorescence to appear in these structures (Fig. 4F; arrow points to mitotic chromatin). Rather, fluorescence is present at the periphery of cells, perhaps because it is displaced elsewhere in the cell by yolk platelets.

BiFC can reveal Smad signalling during normal development

In an effort to ask whether BiFC can be used to assess quantitative aspects of signalling by members of the TGF- β family, we first investigated the extent to which increasing extracellular concentrations of Activin cause increased nuclear accumulation of Smad2-Smad4 complexes. Different concentrations of Activin were therefore added to cultures of dissociated animal cap cells derived from embryos that had been injected with RNA encoding VC155-Smad2 and VNm9-Smad4 BiFC constructs and, to allow normalisation, RNA encoding ECFP (see Materials and methods). The fluorescence intensity in the nucleus after 3 hours of incubation was then quantified with Volocity software and plotted as a ratio of VENUS fluorescence to ECFP (Fig. 5A,B). Our results showed that fluorescence deriving from the accumulation of Smad2-Smad4 complexes became more intense as the extracellular concentration of Activin increased.

These observations suggest that BiFC might be used to monitor levels of Smad signalling during development. To test this idea, *Xenopus* eggs were injected with RNA encoding VNm9-tagged Smad4 together with VC155-tagged Smad2. The large size and yolkeness of *Xenopus* blastomeres precluded direct observation of BiFC fluorescence in the intact embryo, so we dissected early

gastrulae into animal and vegetal halves and studied the two half-embryos. In such embryos, marginal zone cells show nuclear accumulation of Smad2-Smad4 BiFC in a pattern resembling that observed with immunohistochemistry for phosphorylated Smad2

(Schohl and Fagotto, 2002), whereas in the animal hemisphere, as in cells derived from isolated animal pole regions, nuclei are only weakly fluorescent (compare Fig. 5C with nuclear membrane-associated fluorescence in Fig. 4A).

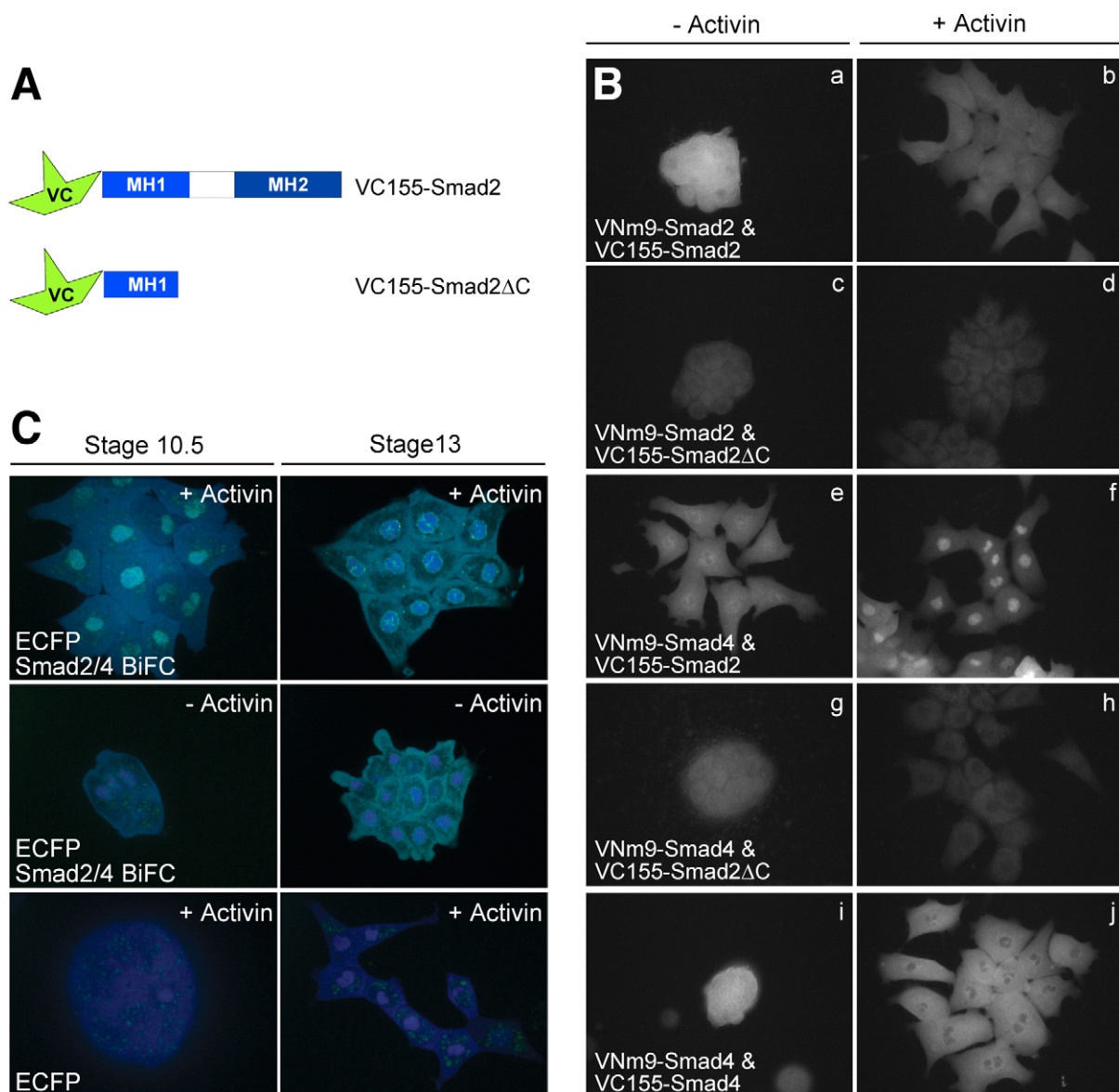


Fig. 3. Smad BiFC constructs respond to Activin signalling. (A) Diagram comparing wild-type VC155-Smad2 with the control protein VC155-Smad2 Δ C. (B) The response of these Smad BiFC constructs to Activin. Embryos were injected at the one cell stage with RNA encoding the indicated BiFC reporter constructs, together with RNA encoding mRFP1 as a lineage marker. Animal pole regions were dissected at the midblastula stage and labelled cells were identified by mRFP1 fluorescence (not shown), disaggregated, and plated on a fibronectin-coated substrate in the presence or absence of Activin. They were cultured to the equivalent of the early gastrula stage. In the absence of Activin (left-hand column of images) cytoplasmic fluorescence is detectable that derives from Smad2 homodimers (a), Smad2-Smad4 heterodimers (e) and Smad4 homodimers (i). Some autofluorescent yolk platelets are detectable in cells expressing VC155-Smad2 Δ C rather than VC155-Smad2 (c,g). Note that levels of fluorescence in these samples is exaggerated because the cells are round; Activin treatment (right-hand column of images) causes cells to flatten (Smith et al., 1990). We note that some flattening also occurs in cells co-injected with RNA encoding Smad2 and Smad4 fusion proteins (see Fig. 2B). In the presence of Activin there is slight accumulation of Smad2 homodimers in the nucleus of responding cells (b) and dramatic accumulation of Smad2-Smad4 heterodimers (f). Smad4 homodimers are excluded from the nucleus (j). Little fluorescence is detectable in cells expressing VC155-Smad2 Δ C rather than VC155-Smad2 (d,h). (C) Loss of nuclear BiFC fluorescence by late gastrula stage 13. Animal pole blastomeres were isolated from embryos that had been injected with RNA encoding VC155-Smad2 and VNm9-Smad4 together with RNA encoding ECFP, or from embryos expressing just ECFP. Dissociated blastomeres were left untreated or treated with 16 U/ml Activin for 10 minutes and then cultured on a fibronectin-coated substrate and observed at the equivalent of stage 10.5 or stage 13. Strong nuclear BiFC fluorescence in response to Activin is detectable at stage 10.5, but by stage 13 this has decreased to the levels observed in untreated cells. Fluorescence levels in cells not expressing Smad-BiFC constructs are shown for comparison.

Fig. 4. Association of Smad2-Smad4 heterodimers with nuclear membranes in interphase cells and with chromatin in mitotic cells.

(A) Cells derived from an embryo expressing VC155-Smad2 and VNm9-Smad4 cultured in the absence of Activin. There are weak strands of BiFC fluorescence in the cytoplasm and around the nucleus. Blue staining derives from co-expressed ECFP lineage tracer that tends to accumulate slightly in the nucleus.

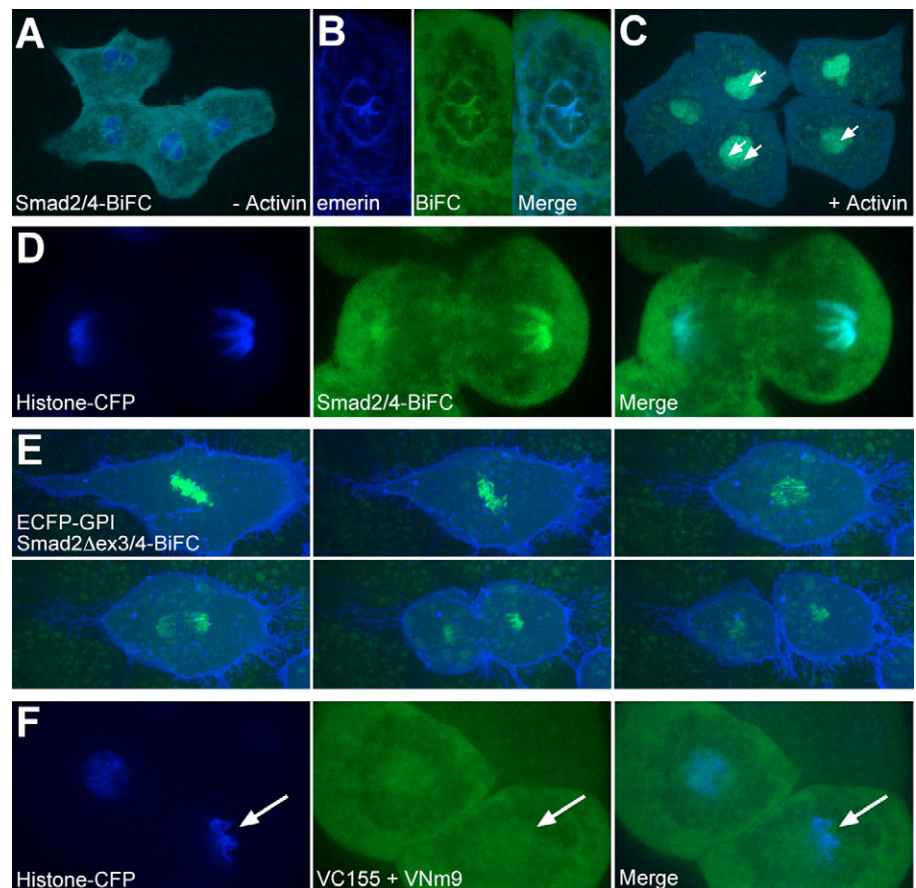
(B) Strands of BiFC nuclear fluorescence in untreated animal pole cells are colocalised with nuclear membranes. Left-hand panel shows staining of ECFP-tagged emerin, middle panel shows BiFC fluorescence, and right-hand panel shows the merged image.

(C) Cells identical to those in A but treated with Activin. Note strong nuclear fluorescence. Arrows indicate spots referred to in text.

(D) Three images of a mitotic *Xenopus* animal pole blastomere derived from an embryo injected at the one cell stage with RNA encoding ECFP-tagged histone H2B (specific fluorescence visible in left-hand panel) and RNA encoding VNm9-Smad4 and VC155-Smad2 (specific fluorescence visible in centre panel). Note that histone and BiFC fluorescence colocalise (right-hand panel). **(E)** Smad complexes are associated with chromatin during mitosis. The cell illustrated is derived from an embryo injected with BiFC constructs designed to reveal heteromeric interactions between molecules of Smad2 Δ exon3 and Smad4.

Images were taken at intervals of 1.5 minutes. Note fluorescence associated with chromatin. Cells co-express an ECFP-GPI membrane marker.

(F) Localisation of Smad-BiFC complexes to nuclear membranes and chromosomes is specific. Injection of RNA encoding the complementary VENU fragments VC155 and VNm9 (200 pg of each, representing a 20 fold molar excess over concentrations used in Smad-BiFC experiments) reveals weak fluorescence in the cytoplasm and at the periphery of cells, but not in the nuclei or on chromosomes. Arrows indicate mitotic chromatin. Higher levels of fluorescence at the periphery of cells may be due to displacement of material by yolk platelets.



Smad2 and Smad4 form a complex only after the midblastula transition

In the course of experiments analysing the speed with which Smad2-Smad4 complexes translocate to the nucleus after treatment with Activin, we noted that such accumulation occurs only after the midblastula transition (MBT), which occurs around stage 8.5 in embryos of *Xenopus laevis* (Newport and Kirschner, 1982b). Thus, addition of Activin to dissociated animal cap cells after the MBT caused detectable accumulation of Smad2-Smad4 complexes within 10 minutes (Fig. 6Af), whereas treatment at any time before the MBT does not result in nuclear accumulation of BiFC signal until control embryos reach stage 8.5 (Fig. 6Aa-d).

The delay in the appearance of Smad2-Smad4 complexes in the nuclei of cells treated with Activin before the MBT is of great interest. It suggests that the time of onset of target gene expression in response to Activin, which is subject to similar temporal regulation (Fig. 6B), may be controlled by the nuclear import of Smad complexes. The temporal regulation we observe (Fig. 6A) is unlikely to be an artefact of our experimental system. First, it cannot derive from a delay in complex formation between the two halves of our mutated VENUS protein, because cytoplasmic fluorescence is clearly visible as early as stage 7 in embryos injected with RNA encoding VC155-tagged Smad2 and VNm9-tagged Smad4 (Fig. 6C). Second, as is observed with the endogenous protein (Fig. 6D)

(Lee et al., 2001), phosphorylation of VC155-Smad2 occurs within 30 minutes of treatment with Activin (Fig. 6E). In this respect we note that the effects of Activin differ from those of the Xnr proteins, which cannot cause phosphorylation of Smad2 until after the MBT (Lee et al., 2001).

Together, these observations suggest that although Activin can cause the phosphorylation of Smad2 as early as stage 7, Smad2-Smad4 complexes are prevented from accumulating in the nucleus until after the MBT. We discuss this phenomenon below.

DISCUSSION

Bimolecular fluorescence complementation reveals interactions between Smad proteins

Bimolecular fluorescence complementation (BiFC) is a powerful technique that can reveal protein-protein interactions *in vivo* and in real time (Hu et al., 2002; Hu and Kerppola, 2003), and which does not require the sophisticated equipment needed for techniques such as fluorescence resonance energy transfer (FRET). In this paper we use this approach to study the TGF β signal transduction pathway, and in particular the association of Smad2 and Smad4 with themselves and with each other. Our results show that our Smad BiFC constructs can be used to reveal homodimerisation and heterodimerisation of Smad molecules during early amphibian development.

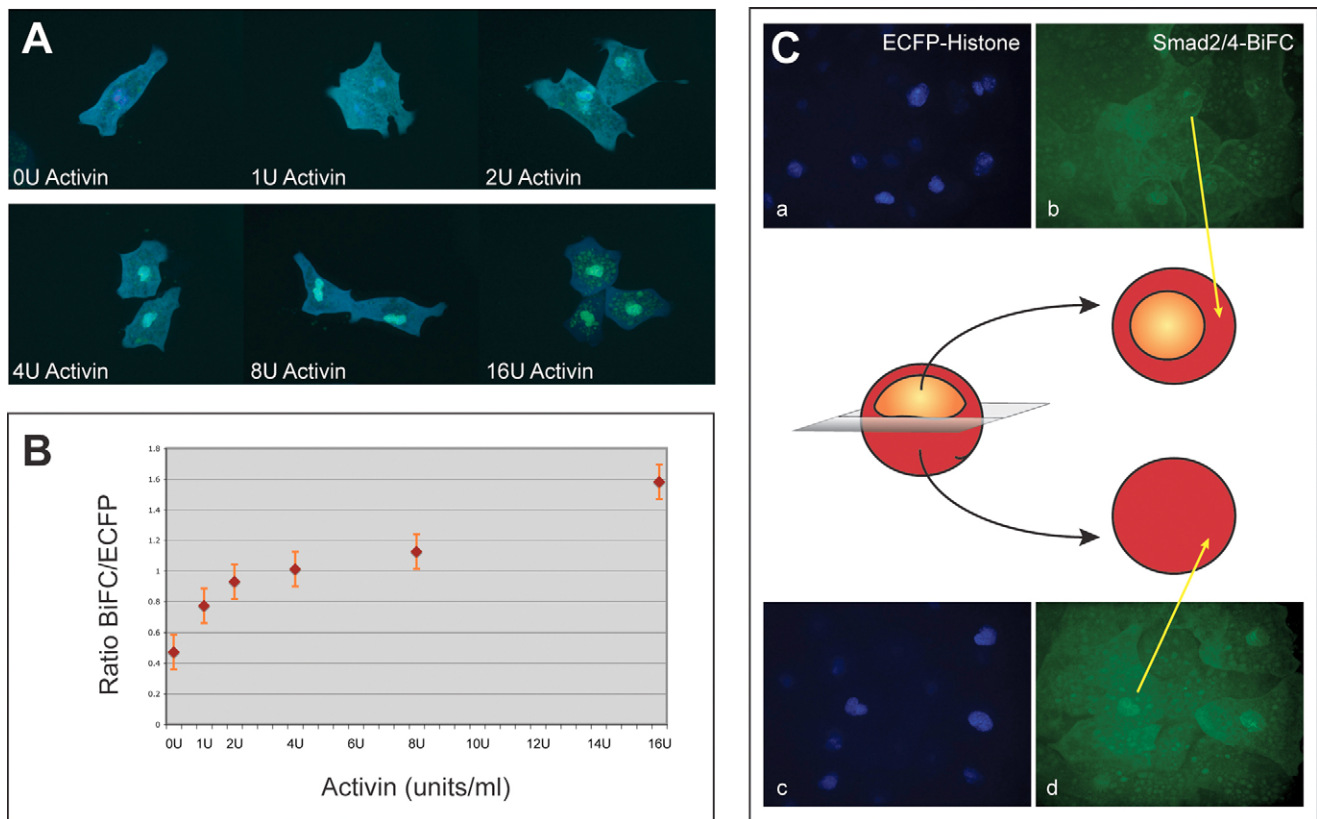


Fig. 5. BiFC Nuclear fluorescence increases as the concentration of Activin is increased; BiFC can reveal endogenous TGF- β signalling during normal development of *Xenopus*. (A) Animal pole blastomeres derived from an embryo injected with RNA encoding VNm9-Smad4 and VC155-Smad2, together with RNA encoding ECFP, were exposed to the indicated concentrations of Activin [measured in units/ml (Cooke et al., 1987)] and examined by fluorescence microscopy 4 hours later. Note that as the concentration of Activin increases, nuclei become brighter. Cytoplasmic fluorescence in cells treated with 16 U/ml activin derives from yolk platelets. (B) Quantification of the data in A. The values represent the ratio of nuclear BiFC fluorescence to ECFP fluorescence in the nucleus averaged over 10-15 cells. The error bars represent standard deviations. (C) Endogenous TGF β signalling in the *Xenopus* embryo revealed by BiFC. *Xenopus* embryos were injected with 100 pg RNA encoding VNm9-Smad4 and VC155-Smad2 together with RNA encoding ECFP-tagged histone H2B. They were cultured to the early gastrula stage before being bisected, as shown in the diagram, into animal and vegetal halves and observed under the fluorescence microscope. Note low levels of fluorescence largely confined to nuclear membrane in the animal hemisphere of the embryo, and higher levels in the nuclei of cells in the vegetal region.

Formation and subcellular distribution of Smad complexes

We have shown that in the absence of Activin, BiFC reveals homomeric interactions between Smads2 and Smads4 and heteromeric interactions between Smad2 and Smad4 in the cytoplasm of *Xenopus* animal pole blastomeres. Although gel filtration experiments do show that Smad2 is present as part of a high molecular mass complex in untreated HaCaT cells (Jayaraman and Massague, 2000), our results contrast with previous reports that Smad2-Smad4 interaction can only be detected after Activin stimulation. However, we note that these conclusions were based on co-immunoprecipitation assays, and they cannot exclude the possibility of transient interactions, which may be stabilised to some extent by the BiFC technique (Kerppola, 2006). Indeed, we note that Smad2 and Smad4 can form homo- or hetero-oligomers in yeast two-hybrid assays (Hata et al., 1997), where there is no ligand-induced phosphorylation at the C-terminus of Smad2. Weak fluorescence, associated with the formation of complexes containing Smad2 and Smad4, was detectable in the nuclei of cells that had not been treated with Activin. This fluorescence was present in nuclear membranes that were marked using ECFP-tagged emerlin (Fig. 4B),

although its significance is not completely clear, because we cannot exclude the possibility that these cells are experiencing very low doses of endogenous TGF β signalling that are not sufficient to induce detectable target gene expression in our assays (see Fig. 2B: 'caps'). We also note that similar perinuclear accumulation of Smad3 was observed in an in vitro nuclear import assay when no active cytosolic factors for nuclear import were added (Kurisaki et al., 2001).

Activin treatment of cells expressing our Smad BiFC constructs causes the rapid nuclear accumulation of complexes containing both Smad2 and Smad4, and of complexes containing two molecules of Smad2 (Fig. 3Bb,f). No change in the distribution of complexes containing two molecules of Smad4 was observed on Activin treatment (Fig. 3Bj).

Our conclusion that homomeric interactions occur between Smad2 and Smad4 is consistent with the observation that TGF β can stimulate the formation of a complex comprising two Smad2s, one Smad4 and one FoxH1 (Inman and Hill, 2002), and with structural analyses showing that the Smad4 MH2 domain can form a homotrimer (Qin et al., 1999). However, our results (Fig. 2C) also indicate that in the presence of Activin, Smad2-Smad4 interactions are

preferred in the nucleus over Smad4-Smad4 interactions, whereas in the cytoplasm of untreated cells Smad4-Smad4 interactions may predominate. Homomeric interactions between Smad4s may therefore play a significant role in the regulation of TGF- β signalling by limiting the availability of Smad4 for heteromer formation with Smad2.

Finally, we note that in mitotic cells, all combinations of Smads associate with chromatin, whether or not Activin is present. This may represent a way of ensuring the equal distribution of Smad proteins to daughter cells (Fig. 4D,E). Our observation differs from previous work suggesting that Smad2 colocalises with microtubules during mitosis (Batut et al., 2007; Dong et al., 2000).

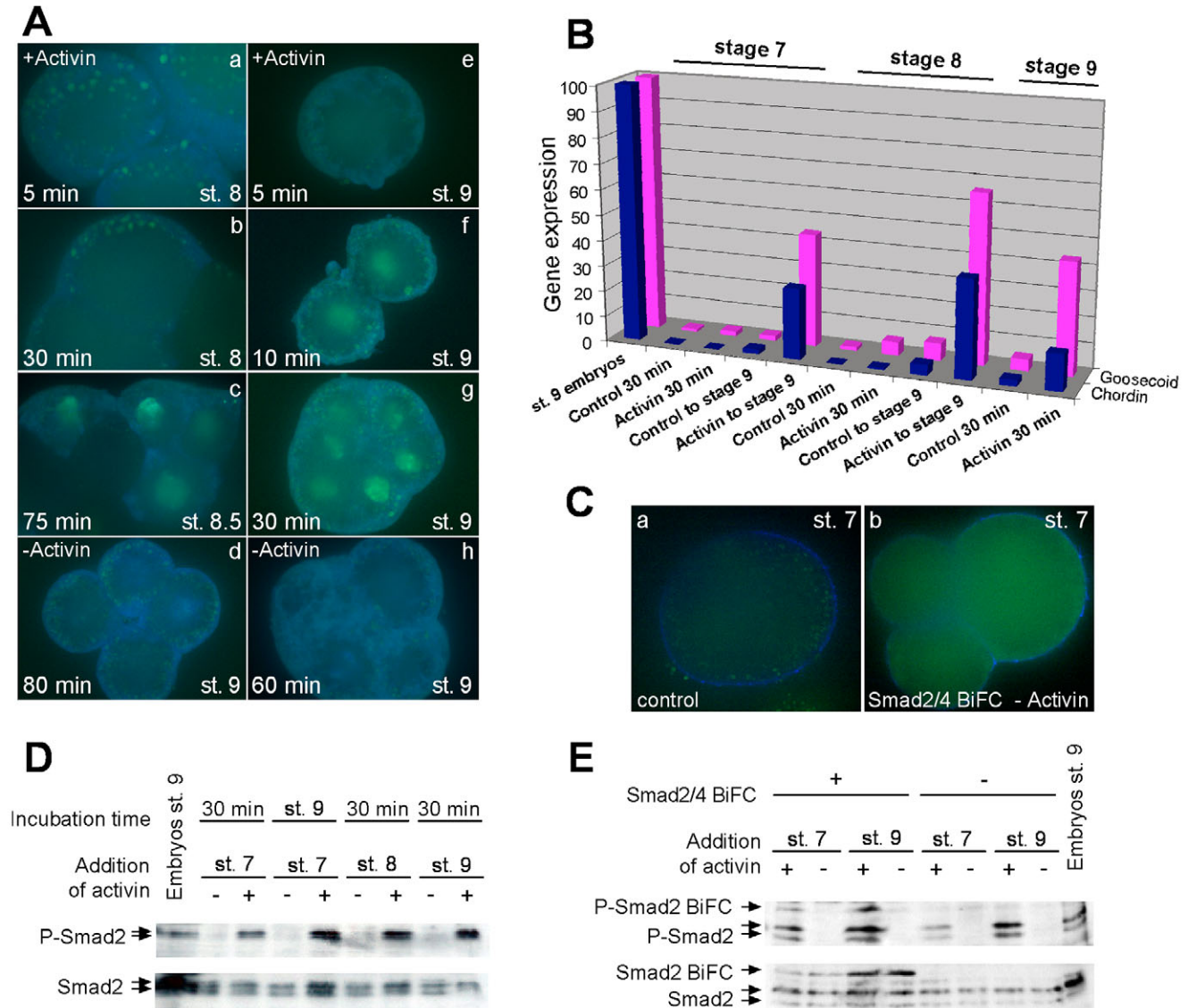


Fig. 6. Entry of Smad2-Smad4 complexes into the nucleus does not occur until the midblastula transition, irrespective of the stage of treatment with Activin. (A) Animal pole cells derived from embryos injected with RNA encoding VNm9-Smad4 and VC155-Smad2 and ECFP lineage marker were treated with Activin at early blastula stage 7 (left-hand column) or late blastula stage 9 (right-hand column), and were cultured for the indicated times. Note that nuclear translocation of Smad complexes in cells treated with Activin at stage 7 occurs only at 75 minutes after treatment, corresponding to stage 8.5 (c), but that the delay in cells treated with Activin at stage 9 is less than 10 minutes (f). (d,h) Control cells that were not treated with Activin. (B) Gene activation in response to Activin also only occurs after stage 9. Animal pole regions were dissected from *Xenopus* embryos at stage 7, 8 or 9 and cultured in the presence or absence of Activin for either 30 minutes or until control embryos reached stage 9 before being assayed for expression of chordin and goosecoid. Following treatment at stage 7, gene activation does not occur within 30 minutes of culture, but is clearly detectable by stage 9. The same is true of animal caps treated at stage 8, but treatment of animal pole regions at stage 9 results in gene activation within 30 minutes. (C) Lack of nuclear BiFC in embryos at stage 7 is not a consequence of the slow maturation of BiFC constructs or delayed complex formation. Compared with uninjected cells (a), weak cytoplasmic fluorescence is clearly visible in cells expressing VC155-Smad2 and VNm9-Smad4 as early as stage 7 (b). (D) Phosphorylation of endogenous Smad2 occurs within 30 minutes of treatment with Activin even at stage 7. The western blot was performed with protein extracts of animal pole regions at the indicated stages. (E) VC155-Smad2 is expressed and can be phosphorylated in response to Activin as early as stage 7. Positions of VC155-Smad2 and of endogenous Smad2 are indicated. Protein extracts are derived from animal pole regions excised from embryos previously injected with RNA encoding VC155-Smad2 and VNm9-Smad4.

Use of Smad BiFC in the analysis of early development

In this investigation we have used BiFC to follow the temporal aspects of Smad signalling in response to the mesoderm-inducing factor Activin. We have shown that the technique is sensitive, quantitative, and, importantly, rapid: complexes containing Smad2 and Smad4 accumulate in the nucleus just 10 minutes after Activin treatment (Fig. 6A). This delay is shorter than that observed with GFP-Smad2 (Bourillot et al., 2002), perhaps because our approach provides a better signal-to-noise ratio. Remarkably, however, the earlier cells are treated with Activin, the longer it takes for BiFC to occur, and we conclude that accumulation in the nucleus can only occur after the MBT (Fig. 6). This delay in the translocation to the nucleus of Smad2-Smad4 complexes is not any consequence of the sensitivity of our assay, because the BiFC constructs are expressed and cytoplasmic Smad2-Smad4 fluorescence can readily be observed as early as stage 7 (Fig. 6C,E). It is also not due to any failure of the animal pole blastomeres to phosphorylate our tagged Smad2; as with the endogenous protein, phosphorylation is clearly detectable within 30 minutes of Activin treatment (Fig. 6D,E).

Our observation may be relevant to the fact that the time of gene activation, or even of morphogenetic movements (Symes and Smith, 1987), in response to Activin depends not on when cells receive an inductive signal, but on the 'age' of the responding tissue (Cooke and Smith, 1990). The observation may even relate to the midblastula transition itself (Newport and Kirschner, 1982a; Newport and Kirschner, 1982b), in the sense that gene activation may not occur until transcription factors, or transcription factor complexes, have gained access to the nucleus. Preliminary results indicate that a fusion protein consisting of cyan fluorescent protein fused to three basic nuclear localisation signals (NLS) also only entered the nucleus after the midblastula transition (see Fig. S1 in the supplementary material). Together, these results suggest, consistent with data of Dreyer (Dreyer, 1987), that the entry of many proteins into the nucleus may be suppressed until MBT in *Xenopus*. We are now investigating how general this conclusion might be, and whether it applies to all transcription factors or indeed to all nuclear proteins.

BiFC and other Smads

TGF β signalling plays important roles in the development of *Xenopus* and of most, if not all, multicellular organisms. If one were able to follow the immediate response to TGF β signalling in individual cells and in real time, this would greatly increase our understanding of early development and also of regeneration and disease. We show here that BiFC between Smad2 and Smad4 can indeed be used to reveal TGF β signalling, suggesting that the creation of transgenic lines expressing the two BiFC constructs might be useful in attempts to follow Smad signalling throughout development and adult life. This might also assist in attempts to understand how cells distinguish between different concentrations of TGF β family members to activate the expression of different genes (Bourillot et al., 2002; Green et al., 1992). In principle, the technique should also be applicable to other members of the Smad family, although our efforts to study the other R-Smads that respond to Activin and the Xnrs in the *Xenopus* embryo have not yet met with success. These proteins are Smad3 (Howell et al., 2001), and a shorter isoform of Smad2 that lacks exon 3 (Smad2 Δ exon3) (Faure et al., 2000). In both cases, BiFC complexes with Smad4 are present in the nuclei of *Xenopus* animal pole blastomeres even in the absence of ligand. This behaviour may be related to the ability of the two proteins to bind DNA directly and to the fact that their nuclear localisation sequences, unlike that of Smad2, are not masked in any

way (Kurisaki et al., 2001). We also note that a GFP-tagged version of Smad3 is constitutively nuclear (Nicolas et al., 2004). In future work we plan to ask whether mutated versions of Smad3 and Smad2 Δ exon3 might provide more effective reagents, and whether one can apply BiFC to Smad1, 5 or 8, which respond to members of the BMP family.

We thank Caroline Hill (CR-UK) and present and former members of our laboratory, especially Shankar Srinivas and Steve Harvey, for their helpful comments. We also thank Andrea Brand, Caroline Hill, Chris Hutchison, Steve Jackson, Atsushi Miyawaki and Oliver Nentwich for cDNA constructs. This work is supported by the Wellcome Trust, the European Union Network *Cells into Organs* and the Foundation for Science and Technology (FCT), Portugal. A.H. is a student of the Gulbenkian Ph.D. Program in Biomedicine, Portugal.

Supplementary material

Supplementary material for this article is available at <http://dev.biologists.org/cgi/content/full/134/23/4209/DC1>

References

- Armes, N. A. and Smith, J. C. (1997). The ALK-2 and ALK-4 activin receptors transduce distinct mesoderm-inducing signals during early *Xenopus* development but do not co-operate to establish thresholds. *Development* **124**, 3797-3804.
- Batut, J., Howell, M. and Hill, C. S. (2007). Kinesin-mediated transport of Smad2 is required for signaling in response to TGF-beta ligands. *Dev. Cell* **12**, 261-274.
- Bengtsson, L. (2007). What MAN1 does to the Smads. TGFbeta/BMP signaling and the nuclear envelope. *FEBS J.* **274**, 1374-1382.
- Bourillot, P. Y., Garrett, N. and Gurdon, J. B. (2002). A changing morphogen gradient is interpreted by continuous transduction flow. *Development* **129**, 2167-2180.
- Campbell, R. E., Tour, O., Palmer, A. E., Steinbach, P. A., Baird, G. S., Zacharias, D. A. and Tsien, R. Y. (2002). A monomeric red fluorescent protein. *Proc. Natl. Acad. Sci. USA* **99**, 7877-7882.
- Cho, K. W., Blumberg, B., Steinbeisser, H. and De Robertis, E. M. (1991). Molecular nature of Spemann's organizer: the role of the *Xenopus* homeobox gene goosecoid. *Cell* **67**, 1111-1120.
- Cooke, J. and Smith, J. C. (1990). Measurement of developmental time by cells of early embryos. *Cell* **60**, 891-894.
- Cooke, J., Smith, J. C., Smith, E. J. and Yaqoob, M. (1987). The organization of mesodermal pattern in *Xenopus laevis*: experiments using a *Xenopus* mesoderm-inducing factor. *Development* **101**, 893-908.
- Dong, C., Li, Z., Alvarez, R., Jr, Feng, X. H. and Goldschmidt-Clermont, P. J. (2000). Microtubule binding to Smads may regulate TGF beta activity. *Mol. Cell* **5**, 27-34.
- Dreyer, C. (1987). Differential accumulation of oocyte nuclear proteins by embryonic nuclei of *Xenopus*. *Development* **101**, 829-846.
- Faure, S., Lee, M. A., Keller, T., ten Dijke, P. and Whitman, M. (2000). Endogenous patterns of TGFbeta superfamily signaling during early *Xenopus* development. *Development* **127**, 2917-2931.
- Green, J. B., New, H. V. and Smith, J. C. (1992). Responses of embryonic *Xenopus* cells to activin and FGF are separated by multiple dose thresholds and correspond to distinct axes of the mesoderm. *Cell* **71**, 731-739.
- Grimm, O. H. and Gurdon, J. B. (2002). Nuclear exclusion of Smad2 is a mechanism leading to loss of competence. *Nat. Cell Biol.* **4**, 519-522.
- Gruenbaum, Y., Margalit, A., Goldman, R. D., Shumaker, D. K. and Wilson, K. L. (2005). The nuclear lamina comes of age. *Nat. Rev. Mol. Cell Biol.* **6**, 21-31.
- Hata, A., Lo, R. S., Wotton, D., Lagna, G. and Massague, J. (1997). Mutations increasing autoinhibition inactivate tumour suppressors Smad2 and Smad4. *Nature* **388**, 82-87.
- Heasman, J. (2006). Patterning the early *Xenopus* embryo. *Development* **133**, 1205-1217.
- Howell, M., Mohun, T. J. and Hill, C. S. (2001). *Xenopus* Smad3 is specifically expressed in the chordoneural hinge, notochord and in the endocardium of the developing heart. *Mech. Dev.* **104**, 147-150.
- Hu, C. D. and Kerppola, T. K. (2003). Simultaneous visualization of multiple protein interactions in living cells using multicolor fluorescence complementation analysis. *Nat. Biotechnol.* **21**, 539-545.
- Hu, C. D., Chinenov, Y. and Kerppola, T. K. (2002). Visualization of interactions among bZIP and Rel family proteins in living cells using bimolecular fluorescence complementation. *Mol. Cell* **9**, 789-798.
- Inman, G. J. and Hill, C. S. (2002). Stoichiometry of active smad-transcription factor complexes on DNA. *J. Biol. Chem.* **277**, 51008-51016.
- Jayaraman, L. and Massague, J. (2000). Distinct oligomeric states of SMAD proteins in the transforming growth factor-beta pathway. *J. Biol. Chem.* **275**, 40710-40717.
- Kerppola, T. K. (2006). Design and implementation of bimolecular fluorescence

- complementation (BiFC) assays for the visualization of protein interactions in living cells. *Nat. Protoc.* **1**, 1278-1286.
- Kurisaki, A., Kose, S., Yoneda, Y., Heldin, C. H. and Moustakas, A.** (2001). Transforming growth factor-beta induces nuclear import of Smad3 in an importin-beta1 and Ran-dependent manner. *Mol. Biol. Cell* **12**, 1079-1091.
- Lee, M. A., Heasman, J. and Whitman, M.** (2001). Timing of endogenous activin-like signals and regional specification of the embryo. *Development* **128**, 2939-2952.
- Nagai, T., Sawano, A., Park, E. S. and Miyawaki, A.** (2001). Circularly permuted green fluorescent proteins engineered to sense Ca²⁺. *Proc. Natl. Acad. Sci. USA* **98**, 3197-3202.
- Nagai, T., Ibata, K., Park, E. S., Kubota, M., Mikoshiba, K. and Miyawaki, A.** (2002). A variant of yellow fluorescent protein with fast and efficient maturation for cell-biological applications. *Nat. Biotechnol.* **20**, 87-90.
- Newport, J. and Kirschner, M.** (1982a). A major developmental transition in early *Xenopus* embryos: I. characterization and timing of cellular changes at the midblastula stage. *Cell* **30**, 675-686.
- Newport, J. and Kirschner, M.** (1982b). A major developmental transition in early *Xenopus* embryos: II. Control of the onset of transcription. *Cell* **30**, 687-696.
- Nicolas, F. J., De Bosscher, K., Schmierer, B. and Hill, C. S.** (2004). Analysis of Smad nucleocytoplasmic shuttling in living cells. *J. Cell Sci.* **117**, 4113-4125.
- Nieuwkoop, P. D. and Faber, J.** (1994). *Normal Table of *Xenopus laevis* (Daudin)*. New York: Garland.
- Piepenburg, O., Grimmer, D., Williams, P. H. and Smith, J. C.** (2004). Activin redux: specification of mesodermal pattern in *Xenopus* by graded concentrations of endogenous activin B. *Development* **131**, 4977-4986.
- Qin, B., Lam, S. S. and Lin, K.** (1999). Crystal structure of a transcriptionally active Smad4 fragment. *Structure* **7**, 1493-1503.
- Rekas, A., Alattia, J. R., Nagai, T., Miyawaki, A. and Ikura, M.** (2002). Crystal structure of venus, a yellow fluorescent protein with improved maturation and reduced environmental sensitivity. *J. Biol. Chem.* **277**, 50573-50578.
- Saka, Y. and Smith, J. C.** (2004). A *Xenopus* tribbles orthologue is required for the progression of mitosis and for development of the nervous system. *Dev. Biol.* **273**, 210-225.
- Sawano, A. and Miyawaki, A.** (2000). Directed evolution of green fluorescent protein by a new versatile PCR strategy for site-directed and semi-random mutagenesis. *Nucleic Acids Res.* **28**, E78.
- Schohl, A. and Fagotto, F.** (2002). Beta-catenin, MAPK and Smad signaling during early *Xenopus* development. *Development* **129**, 37-52.
- Shen, M. M.** (2007). Nodal signaling: developmental roles and regulation. *Development* **134**, 1023-1034.
- Shyu, Y. J., Liu, H., Deng, X. and Hu, C. D.** (2006). Identification of new fluorescent protein fragments for bimolecular fluorescence complementation analysis under physiological conditions. *Biotechniques* **40**, 61-66.
- Smith, J. C., Symes, K., Hynes, R. O. and DeSimone, D.** (1990). Mesoderm induction and the control of gastrulation in *Xenopus laevis*: the roles of fibronectin and integrins. *Development* **108**, 229-238.
- Smith, J. C., Price, B. M., Green, J. B., Weigel, D. and Herrmann, B. G.** (1991). Expression of a *Xenopus* homolog of Brachyury (T) is an immediate-early response to mesoderm induction. *Cell* **67**, 79-87.
- Symes, K. and Smith, J. C.** (1987). Gastrulation movements provide an early marker of mesoderm induction in *Xenopus*. *Development* **101**, 339-349.
- Tada, M., O'Reilly, M. A. and Smith, J. C.** (1997). Analysis of competence and of Brachyury autoinduction by use of hormone-inducible Xbra. *Development* **124**, 2225-2234.